Effect of shear force on the separation of double-stranded DNA

Rakesh Kumar Mishra,[1] Garima Mishra,[1] M. S. Li,[2] and Sanjay Kumar[1]
[1]*Department of Physics, Banaras Hindu University, Varanasi 221 005, India*
[2]*Institute of Physics, Polish Academy of Sciences, Aleja Lotnikow 32/46, PL-02-668 Warsaw, Poland*
(Received 1 February 2011; revised manuscript received 30 June 2011; published 23 September 2011)

Using the Langevin dynamics simulation, we have studied the effects of shear force on the rupture of short double-stranded DNA at different temperatures. We show that the rupture force increases linearly with chain length and approaches the asymptotic value in accordance with the experiment. The qualitative nature of these curves remains almost the same for different temperatures but with a shift in the force. We observe three different regimes in the extension of covalent bonds (backbone) under shear force.

DOI: 10.1103/PhysRevE.84.032903 PACS number(s): 87.15.A−, 64.70.qd, 05.90.+m, 82.37.Rs

Intermolecular and intramolecular forces are key to the stability of DNA and biological processes, e.g., transcription, replication, and slippage [1,2]. Up to now, understanding of these forces was possible through indirect physical and thermodynamical measurements such as crystallography, light scattering, and nuclear magnetic resonance spectroscopy [3]. Single-molecule force spectroscopy experiments have directly measured these forces and provided unexpected insights into the strength of the forces driving these biological processes as well as determined various interactions responsible for the mechanical stability of DNA structures [4–7]. With the increasing number of experiments and insights gathered so far, it has become clear that the measurement of molecular interactions depends on not only the magnitude of the applied force, but also how and where the force was applied [7–15].

A major concern is now to understand whether all these interactions contribute at the same moment or they have different lifetimes. In order to understand this, a force has been applied perpendicular to the helix direction (DNA unzipping) and along the helix direction (rupture and slippage), as shown in Fig. 1 [7–16]. In the case of unzipping of double-stranded DNA (dsDNA), the critical force is found to be independent of the length of DNA and the loading rate [8,9]. This may be understood theoretically that at the center point of the fork [Fig. 1(b)], the applied force breaks only one base pair at a time and hence it remains independent of the loading rate and length. However, when a force (up to 65 pN) is applied along the helix direction (shear force), the length of the dsDNA increases and the force-extension $f - x$ curve can be described by the wormlike chain model [17]. In the high-force regime (>65 pN), the dsDNA can be overstretched about 1.7 times the B-form contour length and a phase transition occurs from the B form to a stretched or S form [18–20]. Recently, van Mameren *et al.* studied DNA stretching with or without DNA binding ligands and demonstrated that overstretching comprises a gradual conversion from dsDNA to single-stranded DNA and it should be interpreted in terms of force-induced DNA melting [21].

For short dsDNA, if the applied shear force increases, the dsDNA separates into two single strands at some critical force. This phenomenon has been identified as rupture [6,10]. The unbinding force strongly depends on the pulling end and is much larger than the unzipping force [6,10,14,22]. Neher and Gerland studied the dynamics of dissociation of the two strands and found the expression for the critical force [23]. Expressing the bond energy and the base pairing energy in the form of harmonic oscillators in the ladder model of dsDNA of length L, de Gennes [24] proposed the maximum force required for the rupture

$$f_c = 2 f_1 \left[\chi^{-1} \tanh\left(\chi \frac{L}{2} \right) + 1 \right]. \tag{1}$$

Here f_1 is the force required to separate a single base pair, which is same for the homosequence, and $\chi^{-1} = \sqrt{Q/2R}$ is the de Gennes characteristic length over which differential force is distributed. Here Q and R are the spring constants characteristic of stretching of the backbone and hydrogen bonds, respectively.

Recently, Danilowicz and co-workers [13] systematically studied the DNA rupture by varying the length of dsDNA. The critical shear force is found to increase linearly up to a certain length and approaches the asymptotic value (≈62 pN), which is in good agreement with the de Gennes prediction. It was argued that the covalent bonds (backbone) and the hydrogen bonds involved in the base pairing will be stretched under the applied force. The differential force will approach zero at the length χ^{-1} if one moves in from either side. However, no experimental effort has been made to study the effect of shearing force on the stretching of covalent bonds and hydrogen bonds inside the characteristic length χ^{-1}. Moreover, in the description of the de Gennes model [24] or the subsequently improved model by Chakrabarti and Nelson [25],

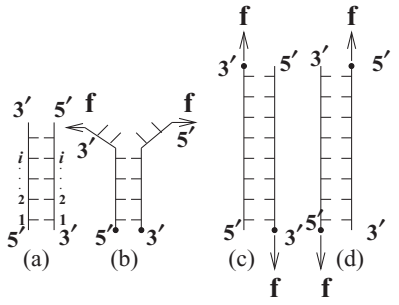

FIG. 1. Schematic representation of dsDNA: (a) dsDNA in zipped form, (b) unzipping of dsDNA by the force f applied at one end ($5' - 3'$), and (c) and (d) shear force along the chain applied at opposite ends ($3' - 3'$ or $5' - 5'$) of the dsDNA.

the effect of thermal fluctuation has been ignored, whereas all the rupture experiments were generally performed at finite temperature. The aim of this Brief Report is to study the effect of temperature T on the rupture and consequences of differential force on the distribution of the extension of bond lengths and hydrogen bonds near the rupture.

We use Langevin dynamics simulation to investigate mechanical and physical properties related to the rupture of DNA [26–29]. Since the rupture time is of the order of milliseconds to seconds, an atomistic simulation of a longer chain in the solvent is computationally difficult [30,31]. We have used a coarse-grained model [7,28,29,32] of the flexible polymer chain to model DNA, which allows us to study a larger system size and events of a longer time scale. A chain in the model consists of bead units connected by effective bonds characterized by stiff springs. Each effective bond represents several chemical bonds (e.g., sugar phosphate) along the chain backbone. The energy of the model system is given by

$$E = \sum_{l=1}^{2}\sum_{j=1}^{N} k\left(u_{j+1,j}^{(l)} - d_0\right)^2 + \sum_{l=1}^{2}\sum_{i=1}^{N-2}\sum_{j>i+1}^{N} 4\left(\frac{C}{u_{i,j}^{(l)\,12}}\right) + \sum_{i=1}^{N}\sum_{j=1}^{N} 4\left(\frac{C}{\left(|\vec{u}_i^{(1)} - \vec{u}_j^{(2)}|\right)^{12}} - \frac{A}{\left(|\vec{u}_i^{(1)} - \vec{u}_j^{(2)}|\right)^{6}}\delta_{ij}\right), \tag{2}$$

where N is the number of beads in each strand and $\vec{u}_i^{(l)}$ represents the position of the ith bead on the lth strand. In present case, $l = 1$ (2) corresponds to first (complimentary) strand of dsDNA. The distance between intrastrand beads $u_{i,j}^{(l)}$ is defined as $|\vec{u}_i^{(l)} - \vec{u}_j^{(l)}|$. The harmonic (first) term with spring constant k (=100) couples the adjacent beads along the two strands. The second term takes care of the excluded volume effect, i.e., two beads cannot occupy the same space [33]. The third term, described by the Lennard-Jones (LJ) potential, takes care of the mutual interaction between two strands. The first term of the LJ potential [which is the same as the second term of Eq. (2)] will not allow the overlap of two strands. Here we set $C = 1$ and $A = 1$. The second term of the LJ potential corresponds to the base pairing between two strands. The base-pairing interaction is restricted to the native contacts ($\delta_{ij} = 1$) only, i.e., ith base of the first strand forms pair with the ith base of the second strand only, as shown in Fig. 1(a). This is similar to the Go model [34]. The parameter d_0 (=1.12) corresponds to the equilibrium distance in the harmonic potential, which is close to the equilibrium position of the average LJ potential. In Eq. (2) we use dimensionless distances and energy parameters. The major advantage of this model is that the ground-state energy of the system is known [34]. The equation of motion is obtained from the following Langevin equation [26,27,29]:

$$m\frac{d^2r}{dt^2} = -\zeta\frac{dr}{dt} + F_c + \Gamma, \tag{3}$$

where m and ζ are the mass of a bead and the friction coefficient, respectively, F_c is defined as $-\frac{dE}{dr}$, and the random force Γ is a white noise [27], i.e., $\langle\Gamma(t)\Gamma(t')\rangle = 2\zeta T\delta(t - t')$. The choice of this dynamics keeps T constant throughout the simulation for a given f. The equation of motion is integrated by using the sixth-order predictor-corrector algorithm with time step $\delta t = 0.025$ [27]. The results are averaged over many trajectories. The equilibration has been checked by monitoring the stability of data against a run that is at least ten times longer. We have used 2×10^9 time steps, of which the first 5×10^8 steps have not been taken in the averaging.

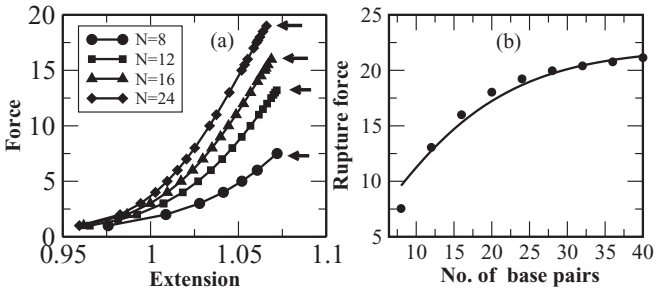

FIG. 2. (a) Force vs extension curves for different chain lengths. Arrows indicate the maximum force, where the number of contacts approaches zero. For the sake of comparison, we have normalized the extension by its contour length (at $f = 0$). (b) Variation of the rupture force with length. The solid line corresponds to a fit to Eq. (1). Solid circles represent the value obtained through the simulation.

In the constant force ensemble, we add an energy $-\vec{f}\cdot\vec{x}$ to the total energy of the system given by Eq. (2). We calculate the reaction coordinate x (extension) for different values of f. The $f - x$ curves [Fig. 2(a)] show the entropic response at low forces and remain qualitatively similar to the one seen in experiments [6,10,11,15]. We identify the rupture force as a maximum force, where the number of intact base pairs suddenly goes to zero. In Fig. 2(b) we show the rupture force as a function of the chain length at low temperature. It is evident from this plot that the rupture force approaches an asymptotic value for a chain length greater than 20, which is in accordance with the experiment [13].

We expand the LJ potential given in Eq. (2) around its equilibrium value. The coefficient of the second (harmonic) term of its expansion corresponds to the elastic constant of the base pairing. The de Gennes characteristic length [24] for the present model is estimated to be ≈10. Substituting the value of f_1 (=1) and the above-mentioned value of χ^{-1} in Eq. (1), we obtain the value of f_c for a given length of dsDNA, which is shown by a solid line in Fig. 2(b). One can notice the good agreement between the simulation and the value predicted by Eq. (1) [24].

One of the important findings of the present simulation is the distribution of stretching of hydrogen bonds Δ_h and the extension of the covalent bonds Δ_c for a wide range of force below the rupture, which are experimentally difficult to obtain. In Fig. 3(a) we depict the variation of Δ_h with base position for the chain of length 40. From this plot one can observe that the hydrogen bonds at extreme ends (up to ≈10 bases) get stretched, whereas bases in the middle (above the de Gennes length ≈10–30) remain the same, indicating that the differential shear force approaches zero in this region. In Fig. 3(b) we show the variation of Δ_c with the base position. All curves have three distinctively different regions. One can observe that bonds near the pulling end (i.e., the 5′ end) get stretched more and decrease gradually. However, when one

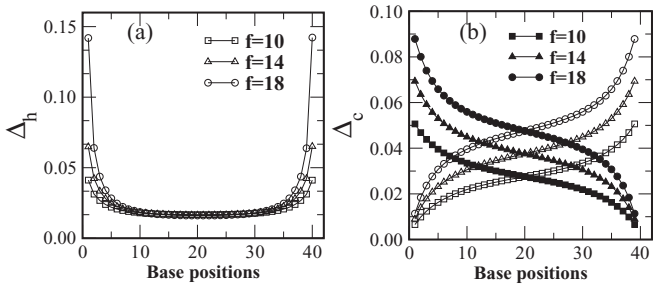

FIG. 3. (a) Variation of the extension of the hydrogen bond length Δ_h along the chain at three different forces. (b) Variation of the extension of the covalent bond length Δ_c along the chain. Open and solid symbols correspond to one strand and its complementary strand, respectively.

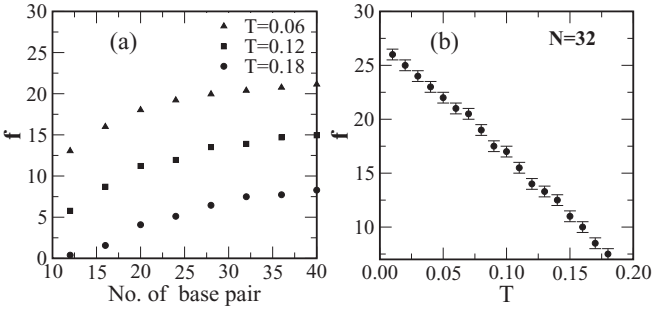

FIG. 4. (a) Variation of the rupture force with chain length at different T. (b) DNA rupture-force–temperature diagram for chain length 32.

approaches the other end (i.e., the 3′ end), there is a change in the slope and the extension is much less than in the middle. It should be noted that 3′ end is near the 5′ end of the other chain, where a similar force is applied. Since dsDNA is in the zipped state, the applied force at the 5′ end of one strand also pulls the other strand along the opposite direction, which causes a relatively slow increase.

In model studies either temperature is set to zero [24] or thermal fluctuation is ignored [25]; as a result, the rupture force defined in Eq. (1) is independent of temperature. However, all rupture experiments are usually performed at room temperature [10,13]; therefore, it is desirable to understand the role of entropy, which may play a significant role at higher T. The thermodynamics of force-induced melting can be obtained from the following relation [35,36]:

$$-fx = \Delta H - T\Delta S, \tag{4}$$

where H is the enthalpy and S is entropy of the ruptured chains. By setting x equal to unity and replacing the value of ΔH by the value of the rupture force at $T = 0$, Eq. (4) can be written as

$$-f = f_c - T\Delta S, \tag{5}$$

where f_c is given by Eq. (1). In the thermodynamic limit, the value of S may be estimated analytically [33] obtained from the experiments [37]. However, for a finite chain length, one must rely on numerical techniques to get the value of S. It is possible to study the effect of temperature on the rupture force in the present setup. In Fig. 4(a) we show the dependence of the rupture force on the length at different temperatures. The qualitative nature of the curves obtained at different T remains similar to the de Gennes plot [Fig. 2(b)], with a shift showing that the rupture force decreases with T. From Fig. 4(a) one can notice that for chain length 32, the rupture force approaches its asymptotic value for all T. In Fig. 4(b) we depict the force-temperature diagram for the DNA rupture for chain length 32. A linear dependence on temperature can be noticed, which is in accordance with Eq. (5). Usually rupture experiments are performed well below the melting temperature, which corresponds to the DNA being in the zipped state. Therefore, in Fig. 4(b) the maximum temperature is set slightly below the melting temperature, i.e., $T_m = 0.23$ at $f = 0$.

In this paper we have studied the effect of shear force and temperature on the rupture of dsDNA. We have shown that the shear force increases linearly with the length of the DNA and then approaches the asymptotic value. In the lattice model, the bond length is constant (stiff); therefore, covalent bonds and hydrogen bonds will not be stretched. As a result, the rupture force increases linearly with length [36] in the lattice model or in models where bond length is considered constant. Our simulations confirm that one will not gain strength by creating a larger pair sequence, as predicted by de Gennes [24]. Interestingly, a recent experiment supports the present work [13]. The distribution of the extension of hydrogen bonds and covalent bonds for different forces is shown in Fig. 3: Fig. 3(a) clearly shows that the increase in the extension of the hydrogen bonds is limited up to the de Gennes length, which is consistent with the strain profile obtained by Chakrabarti and Nelson [25]. Above this length, the differential shear force approaches zero; as a result, there is no extension in the hydrogen bonds. We also find that the qualitative nature of the dependence of the rupture force on length remains the same for different temperatures with a shift. The rupture force decreases with temperature [Fig. 4(b)], as predicted by Eq. (5).

Our study shows that the de Gennes length remains independent of the applied force. The most surprising finding of the present simulation is revealed in Fig. 3(b), which shows a variation of the extension of the covalent bonds along the chain for three different forces ($f = 10$, 14, and 18). In all these cases the differential force approaches zero and there is no relative increase in the bond length above the de Gennes length along the chain [Fig. 3(b)]; however, unlike the hydrogen bonds, there is a net increase in the extension of the covalent bonds, which depends linearly on the applied force. Nuclear magnetic resonance experiments [38] or atomistic simulation [31] should be able to reveal this.

It may be noted that the present simulation is carried out in reduced units. It is possible to extract a rough estimate of the rupture force in real units. The free energy per base pair (including hydrogen bonding and base stacking) of G-C is -1.4 kcal/mol, where stacking accounts for probably half of this amount [39]. Since in A-T base pairing only two hydrogen bonds are involved, one can take approximately two-thirds of the G-C free energy value. To fix the temperature scale one can use DNA melting data where both stacking and hydrogen bonding are required, whereas in rupture, we assume that only

hydrogen bonds are breaking and hence stacking does not contribute significantly. In Ref. [13] heterosequence (50% AT and 50% GC) chains of different lengths were considered. Therefore, we take approximately -0.6 kcal/mol per base of the zipped conformation and equate it with the complete unzipped state. The force required for rupture is found to be approximately 3.5 pN per base pair, which is close to the value used in Ref. [13]. Thus if one scales the y axis of Fig. 2(b) by 3.5 pN, then our results are also in quantitative agreement with the experiment [13].

We thank D. Giri for many helpful discussions on the subject. Financial support from the DST, CSIR, India and the MSI, Poland (Grant No. 202-204-234) is gratefully acknowledged.

[1] B. Alberts *et al.*, *Molecular Biology of the Cell* (Garland, New York, 1994).
[2] J. N. Israelachvili, *Intermolecular and Surface Forces* (Academic, London, 1992).
[3] R. M. Wartell and A. S. Benight, Phys. Rep. **126**, 67 (1985).
[4] S. B. Smith, L. Finzi, and C. Bustamante, Science **258**, 1122 (1992).
[5] P. Cluzel *et al.*, Science **271**, 792 (1992).
[6] G. U. Lee, L. A. Chrisey, and R. J. Colton, Science **266**, 771 (1994).
[7] S. Kumar and M. S. Li, Phys. Rep. **486**, 1 (2010); S. Kumar *et al.*, Phys. Rev. Lett. **98**, 128101 (2007).
[8] B. Essevaz-Roulet, U. Bockelmann, and F. Heslot, Proc. Natl. Acad. Sci. USA **94**, 11935 (1997).
[9] U. Bockelmann, B. Essevaz-Roulet, and F. Heslot, Phys. Rev. Lett. **79**, 4489 (1997).
[10] T. Strunz *et al.*, Proc. Natl. Acad. Sci. USA **96**, 11277 (1999).
[11] I. Schumakovitch *et al.*, Biophys. J. **82**, 517 (2002).
[12] C. Danilowicz *et al.*, Phys. Rev. Lett. **93**, 078101 (2004).
[13] K. Hatch, C. Danilowicz, V. Coljee, and M. Prentiss, Phys. Rev. E **78**, 011920 (2008).
[14] C. Danilowicz *et al.*, Proc. Natl. Acad. Sci. USA **106**, 13196 (2009).
[15] F. Küeher *et al.*, Biophys. J. **92**, 2491 (2007).
[16] S. Cocco, R. Monasson, and J. F. Marko, Proc. Natl. Acad. Sci. USA **98**, 8608 (2001).
[17] J. F. Marko and E. D. Sigga, Macromolecules **28**, 8759 (1995).
[18] M. Rief, H. C. Schaumann, and H. E. Gaub, Nature Struct. Biol. **6**, 346 (1999).
[19] S. B. Smith, Y. Cui, and C. Bustamante, Science **271**, 795 (1996).
[20] J. Morfill *et al.*, Biophys. J. **93**, 2400 (2007).
[21] J. V. Mameren *et al.*, Proc. Natl. Acad. Sci. USA **106**, 18231 (2009).
[22] A. Lebrun and R. Lavery, Nucleic Acids Res. **24**, 2260 (1996).
[23] R. A. Neher and U. Gerland, Phys. Rev. Lett. **93**, 198102 (2004).
[24] P. G. de Gennes, C. R. Acad. Sci. - Ser. IV - Phys. **2**, 1505 (2001).
[25] B. Chakrabarti and D. Nelson, J. Phys. Chem. B **113**, 3831 (2009).
[26] M. P. Allen and D. J. Tildesley, *Computer Simulations of Liquids* (Oxford Science, Oxford, 1987).
[27] D. Frenkel and B. Smit, *Understanding Molecular Simulation* (Academic, London, 2002).
[28] M. Kouza *et al.*, Biophys. J. **89**, 3353 (2005).
[29] M. S. Li, Biophys. J. **93**, 2644 (2007).
[30] T. Hugel, M. Rief, M. Seitz, H. E. Gaub, and R. R. Netz, Phys. Rev. Lett. **94**, 048301 (2005).
[31] M. Santosh and P. K. Maiti, J. Phys. Condens. Matter **21**, 034113 (2009).
[32] J. Schluttig, M. Bachmann, and W. Janke, J. Comput. Chem. **29**, 2603 (2008).
[33] P. G. de Gennes, *Scaling Concepts in Polymer Physics* (Cornell University Press, Ithaca, 1979).
[34] N. Go and H. Abe, Biopolymers **20**, 991 (1981); G. Mishra *et al.*, J. Chem. Phys. **135**, 035102 (2011).
[35] I. Rouzina and V. A. Bloomfield, Biophys. J. **80**, 882 (2001).
[36] A. R. Singh, D. Giri, and S. Kumar, J. Chem. Phys. **132**, 235105 (2010).
[37] J. Santalucia Jr., H. T. Allawi, and P. A. Seneviratne, Biochemistry **35**, 3555 (1996).
[38] W. Saenger, *Principles of Nucleic Acid Structure* (Springer-Verlag, Berlin, 1984).
[39] E. T. Kool, Annu. Rev. Biophys. Biomol. Struct. **30**, 1 (2001).